

Anisotropic glass freezing in rubidium/ammonium dihydrogen phosphate mixed crystal and its deuterated analogue

This article has been downloaded from IOPscience. Please scroll down to see the full text article.

1997 J. Phys.: Condens. Matter 9 4403

(<http://iopscience.iop.org/0953-8984/9/21/007>)

View [the table of contents for this issue](#), or go to the [journal homepage](#) for more

Download details:

IP Address: 171.66.16.207

The article was downloaded on 14/05/2010 at 08:46

Please note that [terms and conditions apply](#).

Anisotropic glass freezing in rubidium/ammonium dihydrogen phosphate mixed crystal and its deuterated analogue

J H Ko[†], B G Kim[†], J J Kim^{†‡§}, H Fujimori[‡] and S Miyajima[‡]

[†] Physics Department and Centre for Molecular Science, Korea Advanced Institute of Science and Technology, Taejon 305-701, Korea

[‡] Institute for Molecular Science, Myodaiji, Okazaki 444, Japan

Received 31 October 1996, in final form 14 February 1997

Abstract. Anisotropic glass freezing has been studied via dielectric measurements in the dipole glass systems of rubidium/ammonium dihydrogen phosphate $\text{RADP}(x)$ and its perdeuterated analogue $\text{D-RADP}(x)$, where x denotes the ammonium concentration. The glass freezing temperatures for a -cut and c -cut crystals are measured, and found to reveal very small anisotropy in the protonated sample of $\text{RADP}(0.43)$ but a considerable anisotropy (~ 7.2 K) at low frequency in the deuterated sample of $\text{D-RADP}(0.40)$. A higher glass freezing temperature was observed along the c -axis as compared with the a -axis freezing temperature for $\text{D-RADP}(0.40)$ crystal. This conforms with the prediction of the cluster model theory for $\text{RADP}(x < 0.5)$. An Arrhenius plot of the logarithmic relaxation frequency versus the reciprocal temperature for $\text{D-RADP}(0.40)$ gave the deuteron activation energies $\Delta E_a \simeq 11.5$ kJ mol⁻¹ along the a -axis and $\Delta E_c \simeq 13.5$ kJ mol⁻¹ along the c -axis.

1. Introduction

Ferroelectric rubidium dihydrogen phosphate (RDP) and antiferroelectric ammonium dihydrogen phosphate (ADP) form a randomly mixed single crystal, $\text{Rb}_{1-x}(\text{NH}_4)_x\text{H}_2\text{PO}_4$ ($\text{RADP}(x)$) over the whole range of x from $x = 0$ to $x = 1$. A dipole glass phase was identified for this system by Courtens [1], and considerable efforts have been devoted to the study of its interesting properties [2–9]. Since dipole glass is formed by frustration and the competing interactions caused by random mixing of the competing interaction units, glass phase formation is common to most of the mixed crystals between ferroelectric alkali hydrogen phosphate or arsenate (often called KDP-type ferroelectrics) and the antiferroelectric ammonium counterparts: deuterated rubidium/ammonium dihydrogen phosphate ($\text{D-RADP}(x)$) [10–15], potassium/ammonium dihydrogen phosphate ($\text{KADP}(x)$) [16–20], rubidium/ammonium dihydrogen arsenate ($\text{RADA}(x)$) [21–23], potassium/ammonium dihydrogen arsenate ($\text{KADA}(x)$) [24], and caesium/ammonium dihydrogen arsenate ($\text{CADA}(x)$) [25], in addition to the prototype $\text{RADP}(x)$. In each of the mixtures, x and $1 - x$ denote the mole fractions of ammonium and alkali ions, respectively. Alkali($1 - x$)/ammonium(x) and phosphate($1 - y$)/arsenate(y) multiple mixing [26, 27] was also studied to examine the dual frustration effects of the randomly competing multiple-Ising-model system.

§ Author to whom any correspondence should be addressed.

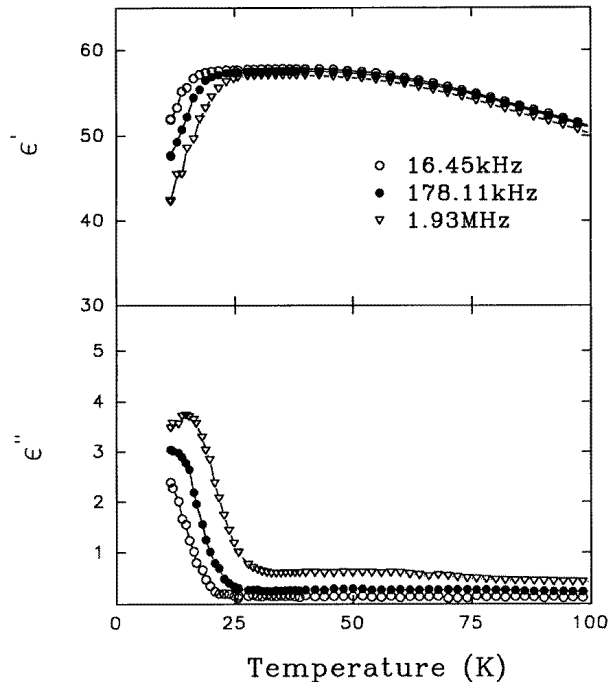


Figure 1. The temperature dependence of the complex dielectric constant, $\epsilon(\nu, T) = \epsilon' - i\epsilon''$, for the *a*-cut specimen of RADP(0.43) at several frequencies. The peak positions of the dielectric loss (ϵ'') curves correspond to the glass freezing temperatures (T_g), which depend on the observation frequency ν .

A number of important features have been revealed for the dipole glass phase: Vogel–Fulcher scaling laws of classical glasses, for example, were found to also hold good for the dipole glass systems [6–7, 10–13]. There are, however, still many problems to be studied to achieve a better understanding of this interesting phenomenon of glass freezing: for example, (i) possible anisotropy in the dielectric susceptibility, which was predicted by the cluster model theory [28–30]; (ii) the nature of the ferroelectric or antiferroelectric phase coexistence with the glass phase; (iii) the roles of the NH_4 and PO_4 ionic dynamics during the glass freezing; and (iv) the effect of deuteration on the glass freezing dynamics. In the present paper we report dielectric studies on single crystals of RADP(*x*) and D-RADP(*x*), and present new results on the dielectric anisotropy observed in the glass freezing of the dipole glass systems, and a significant isotope effect on the anisotropy.

Matsushita and Matsubara [28–30] developed a cluster model theory of dipole glass by incorporating short-range ice-rule correlation for proton configurations (pseudospins), and a Gaussian random distribution for the interaction bonds, and explained the experimental phase diagram successfully, though they neglected dipolar long-range interactions between pseudospin dipoles, and the pseudospin–lattice interactions. An interesting prediction was given on the anisotropy of the dielectric susceptibility tensor χ [30]. The two components, χ_z along the *c*-axis and χ_x along the *a*-axis, were shown to have different relationships with the three order parameters of the glass transition. In particular, for RADP(*x*) crystals with $x < 0.5$, a sharp cusp anomaly was predicted for χ_z at the glass transition temperature (T_g), while a rounded peak appears for χ_x at a temperature below T_g . For the mixed crystals

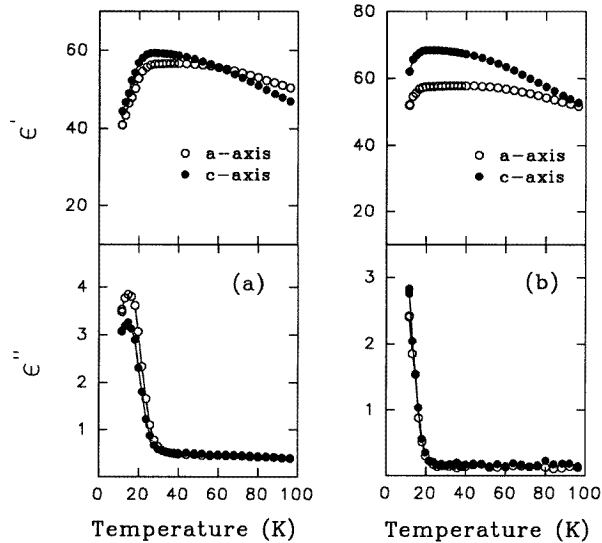


Figure 2. The temperature dependence of the complex dielectric constants for the *a*-cut (○) and *c*-cut (●) crystals of RADP(0.43) observed at (a) 3.105 MHz and (b) 12.96 kHz. The anisotropy in T_g is observed to be less than 1 K for both high (a) and low (b) frequencies.

with $x > 0.5$, it was predicted that only χ_x exhibits a sharp cusp at T_g , while χ_z exhibits a rounded peak at the same temperature T_g .

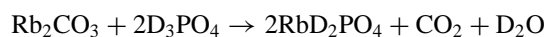
Tunnelling models [31–33] of dipole glass, incorporating dipolar interactions between pseudospins and also the transverse field of tunnelling with random distribution of competing interaction constants, also predict a sharp cusp anomaly of χ at the glass transition temperature T_g . The theories predict a lowering of T_g with increasing tunnelling frequency. The tunnelling frequencies can be increased at high pressure or decreased by deuteration, and corresponding changes of T_g are expected [8, 15]. Anisotropic changes in T_g would also be possible in this model if the tunnelling frequencies become anisotropic as a result of the application of uniaxial high pressure.

Experimentally, the predicted sharp cusps were not observed in RADP(x) [4–11] or D-RADP (x) [11–13] mixed crystals. It was shown later [33, 34] that Gaussian random fields caused by randomly substituted ammonium ions give a rounded peak instead of the sharp cusp, in conformity with the experimental observations. As to the anisotropic dielectric anomaly which corresponds to the anisotropic glass freezing in RADP(x) and D-RADP(x), confusion exists, since a number of research groups reported the absence of anisotropy [9–12], while Stankowski *et al* reported an anisotropic glass transition in D-RADP(x) [35].

It is thus necessary to reexamine the behaviours of dielectric anomalies associated with the glass freezing, and the isotope effects, by using high-precision dielectric data on single crystals.

2. Experimental details

To obtain deuterated mixed crystal, D-RADP(x), the constituent deuterated crystals of D-RDP and D-ADP were prepared by the following chemistry:



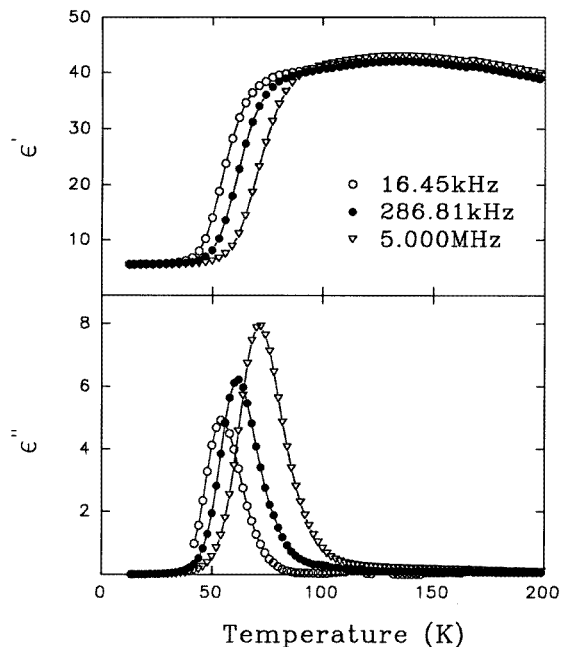
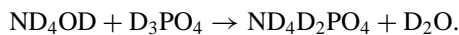


Figure 3. The temperature dependence of the complex dielectric constant for D-RADP(0.40) crystal at 16.45 kHz (○), 286.81 kHz (●), and 5.00 MHz (▽).

and



D-RDP and D-ADP were then mixed in appropriate molar ratios to make saturated solutions in deuterated water. Crystal growth was completed inside a closed vessel to avoid contamination by water vapour in the atmosphere. Specific gravity measurements and proton NMR were used to determine the mole fraction x of ammonium and the percentage of deuteration respectively. Our D-RADP(x) crystal used in the present work was found to have 91% deuteration. The ammonium concentrations were $x = 0.43$ for RADP and $x = 0.40$ for D-RADP.

The dielectric constants of the samples were measured by use of an impedance analyser (HP4192A) in the frequency range from 5 kHz to 5 MHz, and by a lock-in amplifier system employing a function generator and a standard capacitor in the low-frequency region from 1.35 Hz to 5 kHz. Temperature control was achieved by use of a closed-cycle helium refrigerator (Displex) and a personal-computer- (PC-) interfaced temperature controller (Lake Shore-330) with silicon diode temperature sensors. The sample was cooled at a rate of 0.5 to 0.25 K min⁻¹ from above the glass freezing temperature to 10 K.

3. Results and discussion

Figures 1 and 2 show the experimental results for complex dielectric constants, $\epsilon(\nu, T) = \epsilon' - i\epsilon''$, for RADP(0.43) mixed crystal. The real part of the dielectric constant ϵ' starts to deviate from the Curie–Weiss behaviour at the onset temperature of freezing, and then falls rapidly at the low-temperature end of the plateau curve. The temperature of the most rapid

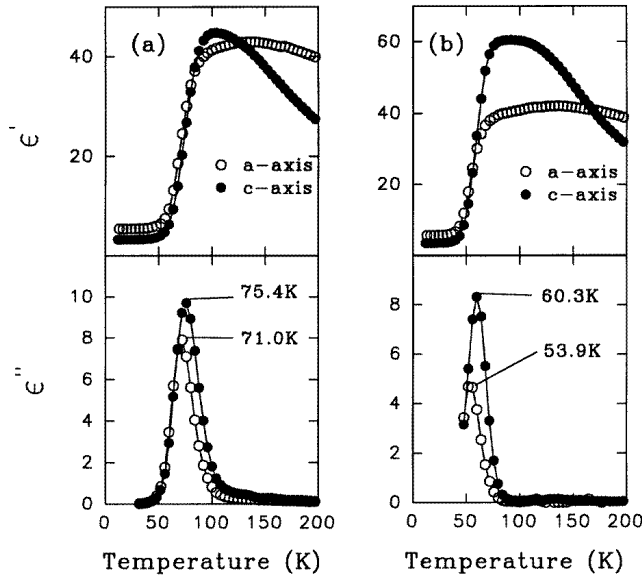


Figure 4. The anisotropy in the dielectric constants of D-RADP(0.40). The complex dielectric constants are shown for the *a*-cut (○) and *c*-cut (●) samples. The observation frequencies are (a) 3.105 MHz and (b) 12.96 kHz.

falling of ϵ' corresponds to the maximum peak of the imaginary part ϵ'' , and is defined as the glass freezing temperature T_g [2]. T_g is clearly dependent on the observation frequency ν , and has already fallen below the lowest attainable temperature (10 K) of our apparatus at a frequency of 16.45 kHz for RADP(0.43). In figure 2 we have compared two dielectric constant curves for *a*-cut and *c*-cut crystal samples of RADP(0.43) measured at 3.105 MHz (a) and 12.96 kHz (b). We can hardly see any significant difference between the values of T_g for *a*-cut and *c*-cut samples of RADP(0.43), in agreement with previous work [9–12]. The possible difference in T_g is estimated to be about 1 K in this frequency range.

In figure 3, temperature and frequency dependences of the complex dielectric constants are shown for a deuterated mixed crystal, D-RADP(0.40). Figure 3 shows the dielectric constant results for *a*-cut sample of D-RADP(0.40) measured at three different frequencies above 16.45 kHz for comparison with figure 1 for the protonated RADP(0.43) sample. The isotope shift of T_g on deuteration can be as large as 55 K in the MHz frequency region, and frequency dependence of T_g could be observed more clearly in this region of higher temperature. In figure 4 we have compared the two sets of dielectric constant data for *a*-cut and *c*-cut samples of D-RADP(0.40) measured at 3.105 MHz (a) and 12.96 kHz (b). In contrast to the case of RADP(0.43) shown in figure 2, T_g is clearly seen to be dependent on the crystal axis of measurement, and is higher when it is measured along the *c*-axis than along the *a*-axis. The difference in T_g is 4.4 K when measured at 3.105 MHz, and 6.4 K at 12.96 kHz. Figure 5 shows the results for dielectric constants measured at $\nu = 1.35$ Hz for the two crystal axes of D-RADP(0.40). The anisotropy in T_g can be as large as 7.2 K at this low frequency. We have thus revealed that larger anisotropy in T_g is observed at lower frequencies of measurement, and this observation is in conformity with the reported value of 4 K at 9.3 GHz [35].

The origin of the anisotropy in the cluster model theory may be traced to the difference

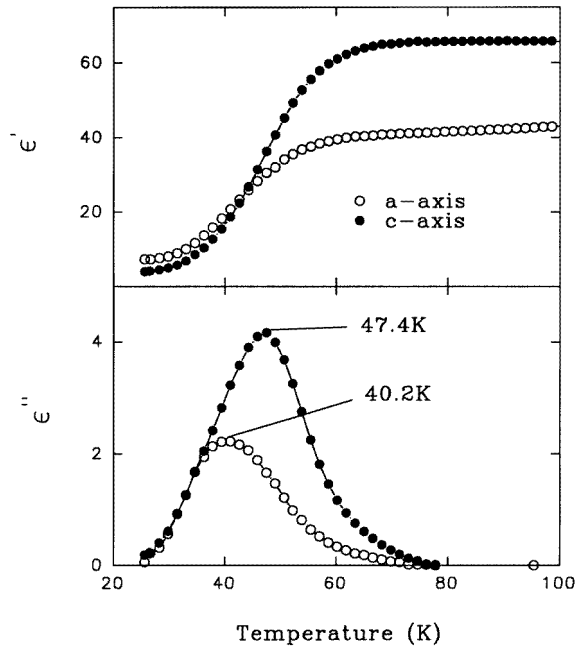


Figure 5. The temperature dependence of the low-frequency ($\nu = 1.35$ Hz) dielectric constant for D-RADP(0.40) crystal, showing very different glass freezing temperatures for the directions along the a - and c -axes of the crystal.

between two effective order parameters [30]:

$$Q_z = \lim_{t \rightarrow \infty} \langle P_z(0)P_z(t) \rangle / \mu^2$$

and

$$Q_x = \lim_{t \rightarrow \infty} \langle P_x(0)P_x(t) \rangle / \mu^2$$

where $P(t)$ stands for a local polarization at time t , and μ stands for the dipole moment of random dipoles. Possible differences between Q_z and Q_x at a given concentration of mixing may originate from the more frequent local cluster formations of ferroelectric- (ΔP_z -) type Slater units for $x < 0.5$ or antiferroelectric- (ΔP_x -) type Slater units for $x > 0.5$. Spatial correlation of the random local clusters (ΔP) will not increase, due to frustration, and will not realize the ferroelectric or antiferroelectric long-range order until the freezing temperature is reached. However, the dynamic autocorrelation, Q_z or Q_x , depending on whether $x < 0.5$ or $x > 0.5$ respectively, will take a nonzero finite value at the freezing temperature, so the corresponding χ_z or χ_x will show a cusp change at this temperature. The minority Slater units—that is, antiferroelectric-type units for $x < 0.5$ or ferroelectric-type units for $x > 0.5$ —will also enter the freezing relaxation at lower temperatures than T_g with more random—that is, single-particle—characteristics of freezing. Our observation of a higher value of T_g in the $\epsilon_c(T)$ measurement than in the $\epsilon_a(T)$ measurement is in conformity with the theoretical prediction of the cluster model for RADP($x < 0.5$) mixed crystal [30].

In figure 6 we have depicted the frequency dependence of the glass freezing temperature T_g as an Arrhenius plot of the logarithmic relaxation frequency versus the reciprocal

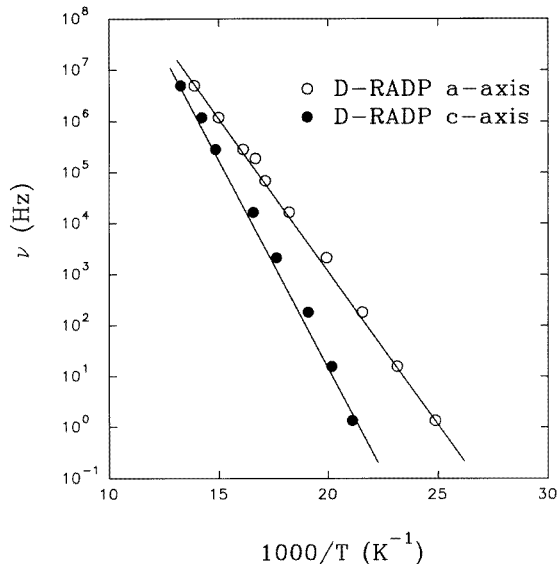


Figure 6. Arrhenius plots of the dependence of T_g on the frequency for the a -axis (○) and the c -axis (●) in D-RADP(0.40) crystal.

temperature for D-RADP(0.40). This picture of the glass freezing as a relaxation rather than an equilibrium transition should give the corresponding anisotropy in the activation energy barrier. The slopes of the two lines give the corresponding activation energy barriers ΔE for the deuteron relaxations along the a -axis (○) and c -axis (●) respectively. We have obtained $\Delta E_a \simeq 11.5 \text{ kJ mol}^{-1}$ along the a -axis and $\Delta E_c \simeq 13.5 \text{ kJ mol}^{-1}$ along the c -axis.

4. Conclusion

The glass freezing temperatures of dipole glass as determined from the dielectric loss peaks are dependent not only on the frequency of a probing field but also on the crystal axis of the dielectric measurement. The crystal axis dependence of the glass freezing temperature—that is, anisotropy in the glass freezing—was observed to be substantial for the deuterated dipole glass D-RADP(0.40), whereas it was very slight for the proton dipole glass RADP(0.43).

It remains a puzzle why a large anisotropy in T_g is observed for deuterated D-RADP(0.40), while the anisotropy is negligibly small for protonated RADP(0.43), although it may be speculated that the short-range anisotropy of the crystal is more susceptible to deuterons in localized single-particle potentials than protons in delocalized extended potentials of 3D correlation, due to more significant zero-point vibration and quantum tunnelling effects.

References

- [1] Courtens E 1982 *J. Physique Lett.* **43** L199
- [2] Courtens E 1987 *Ferroelectrics* **72** 229 and references therein
- [3] Hayase S, Sakashita H and Terauchi H 1987 *Ferroelectrics* **72** 245 and references therein
- [4] Iida S and Terauchi H 1983 *J. Phys. Soc. Japan* **52** 4044
- [5] Courtens E 1984 *Phys. Rev. Lett.* **52** 69

- [6] Takashige M, Terauchi H, Miura Y and Hoshino S 1985 *J. Phys. Soc. Japan* **54** 3250
- [7] Courtens E and Vogt Z 1986 *Z. Phys.* B **62** 143
- [8] Samara G A and Schmidt V H 1986 *Phys. Rev.* B **34** 2036
- [9] Lee K-S and Kim J-J 1986 *J. Phys. Soc. Japan* **55** 4570
- [10] Courtens E 1986 *Phys. Rev.* B **33** 2975
- [11] He P, Deguchi K, Hirokane M and Nakamura E 1990 *J. Phys. Soc. Japan* **59** 1835
- [12] He P 1991 *J. Phys. Soc. Japan* **60** 313
- [13] Kutnjak Z, Filipič C, Levsik A and Pirc R 1993 *Phys. Rev. Lett.* **70** 4015
- [14] Blinc R, Ailion D C, Günther B and Žumer S 1986 *Phys. Rev. Lett.* **57** 2826
- [15] Korner N, Pfammatter C and Kind R 1993 *Phys. Rev. Lett.* **70** 1283
- [16] Ono Y, Hikita T and Ikeda T 1987 *J. Phys. Soc. Japan* **56** 577
- [17] Ono Y, Yamada N and Hikita T 1991 *J. Phys. Soc. Japan* **60** 2673
- [18] Gridnev S A, Korotkov L N, Rogova S P, Shuvalov L A and Fedosjuk R M 1991 *Ferroelectr. Lett.* **13** 67
- [19] Kim J-J and Sherman W F 1987 *Phys. Rev.* B **36** 5651
- [20] Kwon O-J and Kim J-J 1993 *Phys. Rev.* B **48** 6639
- [21] Trybula Z, Stankowski J, Szczepańska L, Blinc R, Weiss A and Dalal N S 1988 *Ferroelectrics* **79** 335
- [22] Trybula Z, Schmidt V H, Drumheller J E, He D and Li Z 1989 *Phys. Rev.* B **40** 5289
- [23] Kim J-J, Kim N and Lee K-S 1988 *J. Phys. C: Solid State Phys.* **21** L663
- [24] Trybula Z, Schmidt V H, Drumheller J E and Blinc R 1990 *Phys. Rev.* B **42** 6733
- [25] Song T K, Moon S E, Noh K H, Kwun S-I, Shin H-K and Kim J-J 1994 *Phys. Rev.* B **50** 6637
- [26] Kim J-J and Shin H-K 1992 *Ferroelectrics* **135** 319
- [27] Kim J-J, Shin H-K and Kwon O-J 1994 *Ferroelectrics* **151** 247
- [28] Matsushita M and Matsubara T 1984 *Prog. Theor. Phys.* **71** 235
- [29] Matsushita M and Matsubara T 1985 *J. Phys. Soc. Japan* **54** 1161
- [30] Matsushita M and Matsubara T 1986 *J. Phys. Soc. Japan* **55** 666
- [31] Pirc R, Tadić B and Blinc R 1985 *Z. Phys.* B **61** 69
- [32] Blinc R and Žekš B 1987 *Ferroelectrics* **72** 193
- [33] Pirc R, Tadić B and Blinc R 1987 *Phys. Rev.* B **36** 8607
- [34] Cowley R A, Ryan T W and Courtens E 1986 *Z. Phys.* B **65** 181
- [35] Stankowski J, Trybula Z and Schmidt V H 1988 *Ferroelectrics* **79** 351